ENG Transactions

Journal homepage: http://www.engtransactions.com

ENG Transactions, vol. 2, pp. 1-18, June 2021
ID: ENGT-2106092112347

Research Article

A Hybrid Diagnostic System to Detect COVID-19 Based on Selected Deep Features of Chest CT Images and SVM

Abdoljalil Addeh[1*], Ali Hemmati[2], Ali Lari[3], Hafiz Mudassir Munir[4]

[1]*Department of Biomedical Engineering, University of Calgary, Calgary, Canada*
[2]*Department of Medical Engineering, Aliabad Katoul Branch, Islamic Azad University, Aliabad Katoul, Iran*
[3]*Electrical Engineering Department, ETS University, Montreal, Canada*
[4]*Electrical Engineering Department, Sukkur IBA University, Pakistan*

Keywords

Early detection,
ConvNet,
COVID-19,
Hybrid diagnostic method,
Optimization algorithm,
SVM.

Abstract

This paper proposes a hybrid diagnostic method for early detection of COVID-19 based on support vector machine (SVM) and selected deep features of chest computed tomography (CT) images. The developed method consists of four main parts including the feature extractor part, feature selection part, classifier part and optimizer part. In the feature extraction part, a convolutional neural network (ConvNet) is implemented for image preprocessing and extraction of new features from CT images. In the feature selection part, minimum Redundancy Maximum Relevance (mRMR) method is applied to select the most effective and informative features for extracted deep features by ConvNet. The selected features are fed into SVM in the classification part. Free hyper-parameters such as size and number of filters in ConvNet, and penalty factor in SVM control their accuracy and robustness. In the optimization part of the developed method, we applied the black widow optimization algorithm (BWOA) for optimal tuning of these parameters. The acquired outcomes demonstrated that the developed diagnostic method has excellent performance in the detection of COVID-19 and distinguishing it from other frequent respiratory illnesses using only small number of training data, which has huge possibility to help physicians and pulmonologist in performing a quick diagnosis. The developed diagnostic method can mitigate the enormous amount of work from professional treatment staff particularly when the healthcare system is overburdened.

1. Introduction

The novel severe acute respiratory syndrome coronavirus, which first emerged in a city of China, Wuhan, in the late 2019, spread quickly throughout the world and led to unprecedented global health and financial crisis. This mysterious disease is titled

* Corresponding Author: Abdoljalil Addeh
E-mail address: abdoljalil.addeh@ucalgary.ca

Received: 11 April 2021; Revised: 28 May 2021; Accepted: 7 June 2021

Please cite this article as: A. Addeh, A. Hemmati, A. Lari, H. M. Munir, "A hybrid diagnostic system to detect covid-19 based on selected deep features of chest ct images and svm", *ENG Transactions*, vol. 2, pp. 1-18, 2021.

COVID-19 and the virus is termed SARS-CoV2. To date (10 December 2020), more than 69 million coronavirus cases have been affirmed, and more than 1.57 M people have died from COVID-19 [1]. The regular clinical features of this deadly disease include low-grade or high-grade fever, nonproductive cough, tiredness, aches and pains, diarrhea, sore throat, chest pain or pressure, headache, dyspnea, and taste/smell loss [2]. Because of the intensive infectivity of COVID-19, prompt and accurate diagnostic methods are urgently required to recognize, isolate and treat the patients immediately [3]. Timely identification and isolation of affected people could reduce the risk of further public contamination and fatality rates significantly.

Real-time reverse transcription-polymerase chain reaction (RT-PCR) is the most commonly known medical examination technique currently used for the diagnosis of COVID-19, which depends on capturing and detecting the virus. However, some patients with a possibly novel coronavirus infection may have initial negative RT-PCR findings, according to recent research papers [4- 6]. Reasons for fake negative RT-PCR tests may involve inadequate cellular material for the detection as well as improper nucleic acid extraction from clinical materials. The low sensitivity of RT-PCR test is unacceptable in the present epidemic situation. In certain cases, it is very difficult to know about infected people and get adequate care on time. Because of the transmissible nature of novel coronavirus, the infected people can have the virus spread to healthy people. In addition, RT-PCR tests need a laboratory, so it is a time-consuming test. These important issues and other disadvantages reduce the trust on RT-PCR test.

Recent studies suggest that radiology-imaging techniques, especially chest computed tomography (CT) images, can provide important and discriminating information about infection caused by COVID-19 virus. In addition, chest CT imaging might show irregularities and abnormalities earlier than RT-PCR examination, based on the findings. Several research findings have shown significant changes in CT scan images prior COVID-19 symptoms started [7, 8]. Chest CT test is fast and easy and has already had successful success in the diagnosis of some of the other coronaviruses [9]. Utilizing chest CT images to detect COVID-19 is therefore not an ideal solution. Radiologists still find it challenging to distinguish between infected and uninfected lungs. Unfortunately, with a visual inspection, this suffers from the unavoidable human mistake and malfunction, which can be further amplified by the low quality of CT images. Furthermore, excellently-trained algorithms in machine learning (ML) can concentrate on points that are not perceptible to the doctor's unaided vision, and therefore can serve to change such a perception [10]. In addition, providing expert clinicians to each and every clinic is a difficult challenge due to a limited number of radiologists, especially in remote areas. Accurate, quick and easy solutions focused on ML-based approaches could therefore be incredibly helpful in tackling this problem and providing patients with timely assistance.

Over the past few years, ML-based approaches have become one of the leading research topics in medical image computing as well as in clinical diagnosis [10-17]. Such intelligent technologies also have great benefits over radiologists. They are reproducible, and hence they identify the subtle changes that visual observation cannot identify. Since the start of the COVID-19 outbreak, several studies have been done on chest X-ray and CT image processing using ML algorithms with the aim of providing a fast and accurate COVID-19 diagnosis method. Most of the developed methods have used convolutional neural networks (ConvNet) as the classifier [18- 33]. As an example, in [18] ten popular ConvNet architectures such as AlexNet, GoogleNet, VGG-19, VGG-16, SqueezeNet, ResNet-18, MobileNet-V2 and Xception were applied to analyze CT images to detect COVID-19 infection. The best performance, 99.51% recognition accuracy is achieved by ResNet-101 architecture. In [19], various common pre-trained ConvNet architectures such as ResNet18, ResNet50, ResNet101, and SqueezeNet were utilized for CT images analysis and COVID-19 detection. In the introduced approach, three levels of decomposition on CT images have been performed [34] by the stationary wavelet transform and also the wavelet output is utilized as the ConvNet architecture's input. Authors in [20] have used a total number of 617,775 CT images from 4154 infected people for implementing and developing a ConvNet based model to diagnose COVID-19 precisely. The proposed technique performs well in identifying some

features such as ground-glass opacities (GGO), interstitial changes with a peripheral distribution, and multifocal patchy consolidation, which shows COVID-19 in the patients' CT images. In [21], combination of ConvNet and Long-Short Term Memory (LSTM) was utilized for COVID-19 detection. In this approach, ConvNet is used for feature extraction from CT images, and LSTM is used for classification purpose. Authors in [22] have utilized 4356 chest CT images obtained from 3322 patients for developing a 3D ConvNet-based model for acquiring a per-exam sensitivity of 90% and a per-exam specificity of 96% in COVID-19 diagnosis from community-acquired pneumonia. Researchers in [23] have gathered 4982 CT slices from 3645 COVID-19 affected people to develop a dual-sampling attention network for COVID-19 detection and distinguish this disease from other similar diseases. The dataset is provided by eight collaborative hospitals. The developed method can detect the COVID-19 images by 87.5% recognition accuracy and 0.944 area under the curve (AUC) value. In [24], researchers have used 132,583 CT image slices form 1186 patients to train a ConvNet. The developed method had 96.00% recognition accuracy with AUC of 0.95.

Although the ConvNet-based detection approaches and systems have satisfactory and favorable specificity and sensitivity, but still using the ConvNet for screening COVID-19 is a challenging task for the researchers. First, most of the available ConvNet-based approaches are applied on relatively large datasets. Acquiring adequate number of CT samples combined with precisely annotated labels require lots of effort and also it is not economical, particularly for some small hospitals in some developing countries. Considering the fact that the race and the COVID-19 mortality rate are strongly related, we will get to know that how serious the situation is. The behavior of COVID-19 varies from community to community. Thus, developing a new diagnostic method which there is no need of large amounts of data is necessary. Secondly, in the ConvNet's structure there exists various hyper-parameters affecting its accuracy. Due to the fact that there are internal relations among these hyper-parameters, they should be optimized and tuned optimally to result in achieving reasonable performance and high accuracy. In most of the COVID-19 diagnostic approaches based on ConvNet, researchers normally have selected these parameters using error and trial, and they are not optimized. Third, most ConvNet models consider the accuracy as the main metric at the cost of more layers, more parameters, and more operations. In a typical ConvNet, most of the weights are in the fully connected layers (FCLs). Inference of ConvNets with large architecture on microprocessors is quite challenging because these devices are usually limited in terms of performance, cost, memory, and energy [35].

Considering the importance of early and accurate detection of COVID-19, a simple, fast and accurate diagnostic method is proposed in this study. In the developed method, we used ConvNet for automatic feature extraction from CT image slices. The convNets have been used in different practical problems due to their excellent feature extraction capability [36- 39]. In order to improve the generalization capability, we used support vector machine (SVM) instead of FCLs. Outstanding generalization capability of SVM makes it different from other classification algorithms. The SVM is one of the few ML algorithms to handle the generalization issue [40]. Recently, nature inspired optimizers have attracted the attention of researchers to solve complex engineering problems[46-48]. Moreover, black widow optimization algorithm (BWOA) is applied to find the optimal hyper-parameters of ConvNet and SVM. The BWOA is one of the most accurate and fast nature-based optimization algorithms that has been introduced recently [41]. For further improvement of recognition accuracy and reduction of computational burden, minimum Redundancy Maximum Relevance (mRMR) feature selection algorithm is implemented to select the most efficient features. The selected features are fed to SVM for final classification. The main contributions of our developed diagnostic method are as follow:

- Designing the ConvNet and SVM with optimal architecture in order to enhance the recognition accuracy
- Selection of the most efficient deep features using mRMR that are more efficient than concatenated deep features, in order to decrease the computational burden and enhance recognition accuracy

- Improving the generalization capability by replacing SVM with FCL

The rest of the article is arranged as follows. Section 2 introduces CT images and their characteristics, and feature selection algorithm. Section 3 presents the proposed method and provides details. In the fourth section, the results of numerical studies and simulations are presented. Section 5 summarizes and concludes the paper.

2. Materials and Methods

2.1 CT Images

Although the RT-PCR test is remarkably specific, its low sensitivity of 65-95 percent indicates that even though the patient is infected, this method may be negative. Another issue is that doctors must wait for the lab results, which could also require around 24 hours or even more than that, while the CT results are instantly available [42, 43]. Chest CT imaging can manifest abnormalities in advance of the RT-PCR approach, by experiences obtained over the recent four months. High-resolution CT is currently included as one of the primary approaches for screening, primary diagnosis, and disease severity assessment. A CT scan is a diagnostic imaging process that utilizes computer-processed combinations of many X-ray measurements collected from different angles to generate cross-sectional (tomographic) images of particular areas of a scanned object, allowing the user to see without cutting inside the object.

The most common finding in COVID-19 infections obtained through chest computed tomography images is the GGO pattern [42]. Figure 1 shows a chest CT-images of an adult female, who had a high fever for a week with shortness of breath and progressive nonproductive coughing. In this case, the RT-PCR test was positive for COVID-19, and saturation at admission was 65 percent. There were broad bilateral GGO with a posterior predominance. Moreover, the broadening of the vessels is a regular finding in the region of ground glass. Figure 2 shows this fact.

In some cases, there are thickening intralobular and interlobular lines as well as a GG model that is called crazy paving (CP). It has commonly been assumed that this model is seen in a slightly later time [43]. Figure 3 shows this fact. Additional frequent discovery in the areas of GGO is traction bronchiectasis [43]. Figure 4 shows this fact. In certain instances, structural deformation with the configuration of subpleural bands is observed that can be seen in Figure 5.

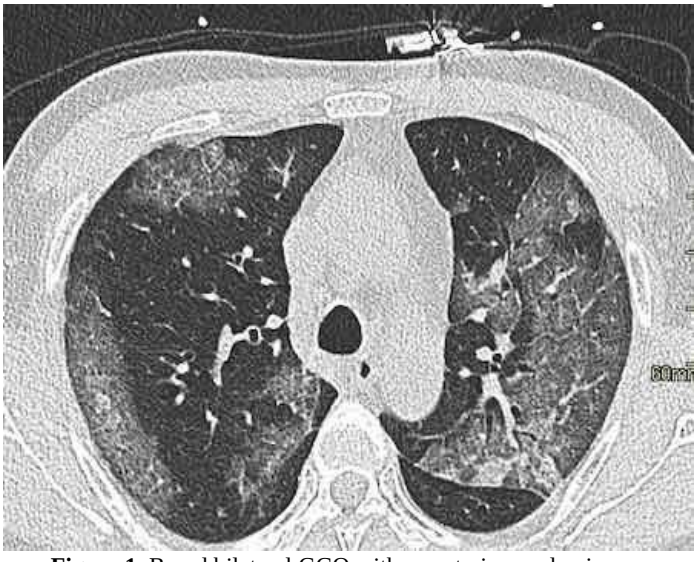

Figure 1. Broad bilateral GGO with a posterior predominance

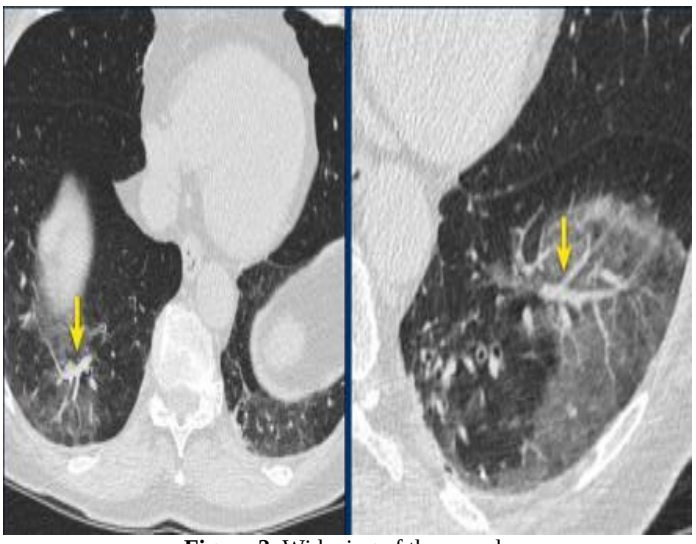

Figure 2. Widening of the vessels

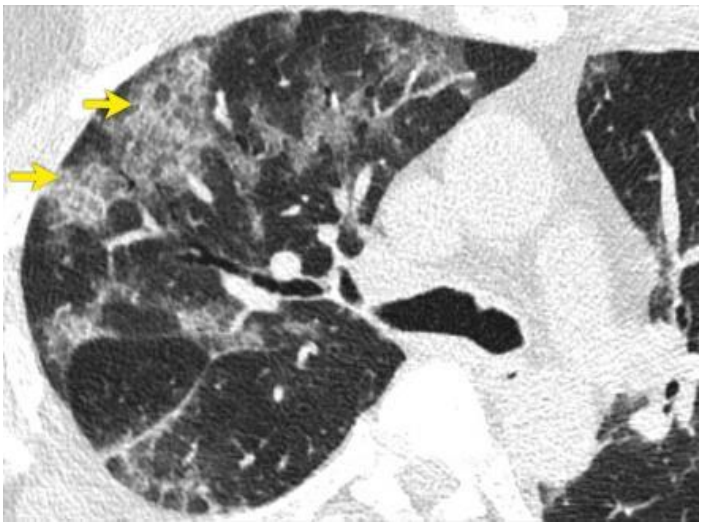

Figure 3. CP pattern in CT images

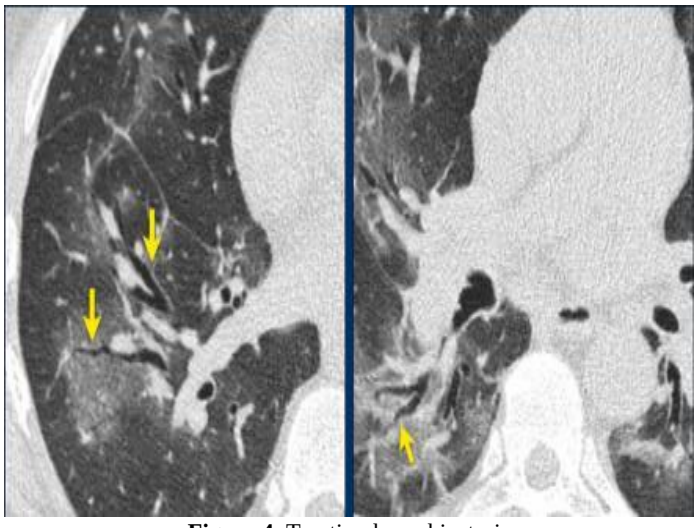

Figure 4. Traction bronchiectasis

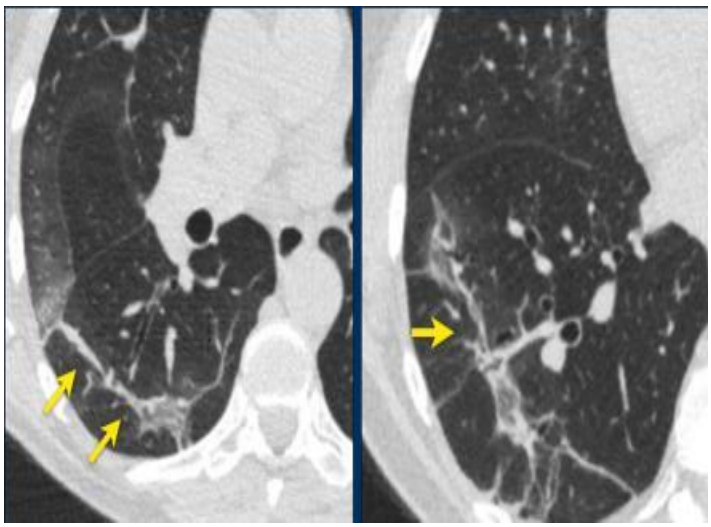

Figure 5. Architectural distortion

Findings achieved by original chest computerized tomography in COVID-19 instances comprise bilateral, multilobar GGO with a posterior or peripheral spread, mostly in the bottom lobes and less commonly distributed in the middle lobe. Also, consolidation superposed on ground-glass opacity as the primary imaging exhibition takes place in a smaller number of samples, largely in patients with higher ages. Some other fewer discoveries through original chest computerized tomography are subpleural involvement, septal thickening, pleural thickening, and bronchiectasis, which are less frequent [42, 43].

2.2 mRMR

This feature selection algorithm is a filtering approach that attempts to reduce redundancy between redundancies of chosen features while attempting to choose the most associated features with class tags. This feature selection algorithm regards each feature as a discrete coincidence variable and employs the mutual information (MI) between them to assess the grade of resemblance between the two features, X and Y, utilizing the $I(X,Y)$ as follow:

$$I(X,Y) = \sum_{y\epsilon Y}\sum_{x\epsilon X}(x,y)log\left(\frac{p(x,y)}{p_1(x)p_2(x)}\right) \quad (1)$$

In Eq. (1), $p_1(x)$ and $p_2(x)$ show the marginal probability distribution function of coincidence variables, and $p(x,y)$ shows the combined probability distribution function of X and Y. To facilitate equation, each feature f_i is explained as a vector shaped by ordering K features ($f_i[f_i^1, f_i^2, f_i^3, \dots, f_i^K]$). The f_i serves as an example of a discrete coincidence variable and MI between i and j features explained as $I(f_i, f_j)$. Where $i = 1,2,\dots,d; j = 1,2,\dots,d$ and d represents the number of feature vector. The concept of MI is used not only for level the of similarity between two features but also for measuring the similarity I(H, f_i) between any feature i and the class labels vector, $h = [h^1, h^2, \dots, h^N]$. Let S be the set of selected features and $|S|$ shows the number of selected features. Two conditions need to be met to ensure that the best features are selected. The first one is termed the minimum redundancy condition:

$$minW, W = \frac{1}{|S|^2}\sum_{F_iF_j\epsilon S} I(F_i, F_j) \quad (2)$$

The other is the maximum relevance condition:

$$\max V, V = \frac{1}{|S|}\sum_{F_i\epsilon S} I(F_i, H) \quad (3)$$

The two simple combinations that combine the two conditions can be denoted by the following equations:

$$max(V - W) \quad (4)$$

$$max(^{V}/_{W}) \tag{5}$$

According to the above equations, since the search algorithm is required to select the best number of feature, primarily, the first feature is selected according to Eq. (3). Then the feature i that provides Eqs. (6) and (7) is selected at each step and this feature is stored in the selected feature set. ohm;$_{s}$ = ohm; −S represents all the features except for selected features:

$$max_{f_{i\epsilon ohm;S}} = I(H, F_i) \tag{6}$$

$$max_{f_{i\epsilon ohm;S}} = \frac{1}{|S|}\sum_{F_i \epsilon S} I(F_i, F_j) \tag{7}$$

The combinations of Eqs. (4) to (6) and (5) to (7) shape two feature selection criteria for the algorithm named Mutual Information Difference (MID) and Mutual Information Quotient (MIQ). The mathematical expression of MID and MIQ are as follow:

$$MID: max_{f_{i\epsilon ohm;S}} \left[I(F_i, H) - \frac{1}{|S|}\sum_{F_j \epsilon S} I(F_i, F_j)\right] \tag{8}$$

$$MIQ: max_{f_{i\epsilon ohm;S}} \left[\frac{I(F_i,H)}{\frac{1}{|S|}\sum_{F_j \epsilon S} I(F_i,F_j)}\right] \tag{9}$$

3. Proposed Method

This paper proposes an intelligent method based on ConvNet and SVM for chest CT image analysis and COVID-19 detection. The proposed method includes four main modules: a feature extraction module, a classification module, feature selection module and an optimization module. Figure 6 shows the main framework of the proposed COVID-19 diagnosis method. In the feature extraction module of the proposed method, we used a ConvNets for generating deep and abstract features from CT images that cannot be seen or detected by a human expert. The automatically extracted features lead to more accurate infection detection and classification. In the feature selection module, mRMR algorithm is applied on extracted deep features by ConvNet. Selection of effective features and removing redundant features lead to higher recognition accuracy and lower computational burden. In the classifier module, we used SVM. The SVMs seem to be effective alternatives to FCL, which conquer some of the fundamental flaw connected to FCL while retaining all advantages of FCL [44].

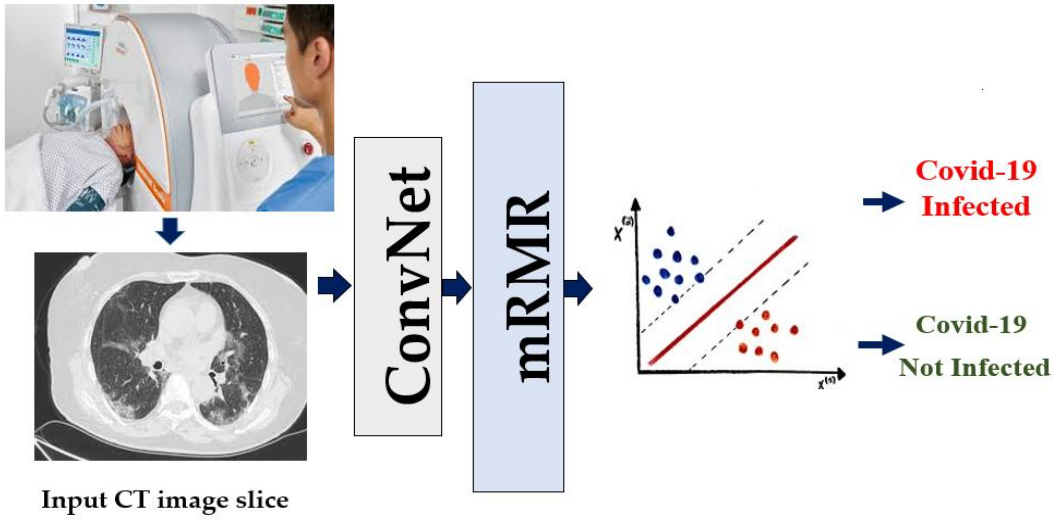

Figure 6. Main framework of the proposed COVID-19 diagnosis method

One great obstacle for implementing any classifier on a new problem is that it requires the amount of considerable experience and skill to select fitting hyper-parameters such as activation function type, number of convolution and pooling layer in ConvNets and kernel type and penalty factor in SVM. Since these hyper-parameters have internal relations, their tuning is notably expensive and time-consuming. For example, the higher number of convolution filters in the convolution layers with small size in ConvNet results in higher precision, but it also makes the training process more difficult due to a too large searching space. In SVM, the behavior of the SVM with Gaussian kernel function is very sensitive to gamma (γ) and penalty factor (C). The gamma determines how far the influence of a single training example reaches and the penalty factor trades off correct classification of training examples against maximization of the decision function's margin. When gamma is very small, the model is too constrained and cannot capture the complexity or "shape" of the data. On the other hand, if gamma is too large, the radius of the area of influence of the support vectors only includes the support vector itself and no amount of regularization with penalty factor will be able to prevent overfitting.

These hyper-parameters in the developed classifier are number of convolution and pooling layer (NL), activation function type (T_{Act}), learning rate (ŋ), number of kernels in convolution layer (NK_C), size of kernels in convolution layer (SK_C), stride value in the convolution layer (S_C), zero-padding value (Z), pooling method type ($T_{pooling}$), size of kernels in pooling layer (SK_P), stride value in the pooling layer (S_P) in ConvNet, and γ and C in SVM. In the developed method, we used Gaussian kernel function in SVM. The T_{Act} could be rectified linear unit (ReLU), randomized ReLU (RReLU) and parametric ReLU (PReLU) and the $T_{pooling}$ could be Mixed, L_P and Spatial Pyramid.

In the developed method, the BWOA is employed for finding the optimal value of hyper-parameters in ConvNet and the SVM network. In the propounded method, the first variable in each spider indicates the number of convolution-pooling layers in ConvNet, the second variable indicates the learning rate, and the third and fourth variables show γ and C in the SVM. The reaming variables indicate the hyper-parameters of each convolution layer and the pooling layer. Figure 7 shows unknown hyper-parameters in the proposed method.

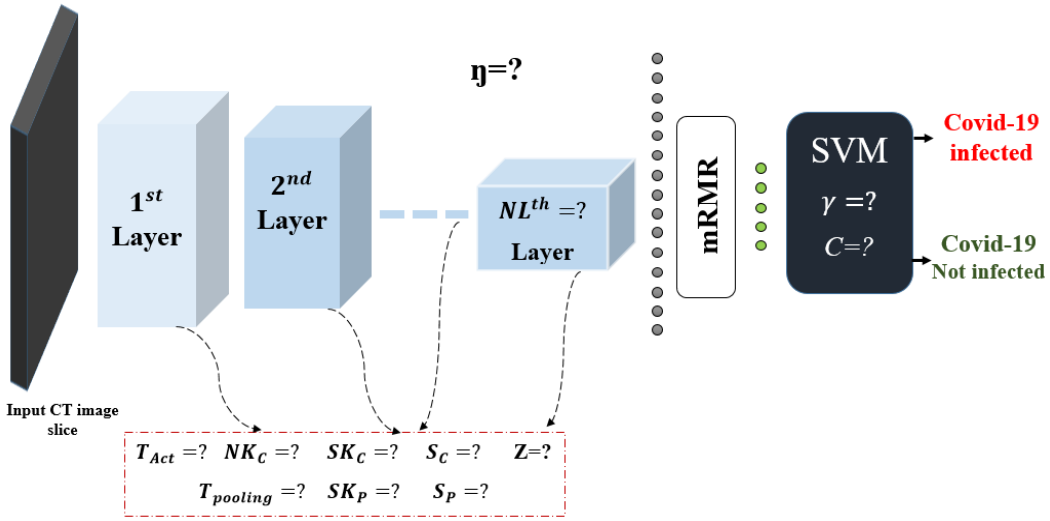

Figure 7. Unknown hyper-parameter values in the proposed classifier

One of the critical challenges in the optimization task is defining a suitable fitness function. Recognition accuracy, which is calculated through confusion matrix, has been utilized as the fitness function of the BWOA in our developed method. The confusion matrix consists of four entries, namely: True positive (TP), False positive (FP), True negative (TN) and False negative (FN). In this matrix, TP refers to the cases' number which has been classified accurately when COVID-19 infected, FP refers to

the cases' number which has been classified incorrectly when COVID-19 infected, TN refers to the cases' number which has been classified correctly when COVID-19 not-infected (healthy) and FN refers to the cases' number classified incorrectly when COVID-19 not-infected (healthy). Recognition accuracy refers to a test's capability in differentiating between COVID-19 infected patients and not infected cases in an accurate way. For estimating a test's recognition accuracy, the proportion of TP and TN in all of the cases which have been evaluated need to be calculated. Mathematically, this can be formulated as below:

$$\text{Fitness function:}\quad \text{Recognition accuracy}=\frac{\text{TP+TN}}{\text{TP+FN+FP+TN}}\times 100 \tag{10}$$

An ideal medical test should show a positive result for all cases who have the target condition (in this study, COVID-19 infected condition). Its capability to do this is stated by its sensitivity. Sensitivity is the proportion of all patients with the disease (TP + FN) who indeed have a positive test result (TP). However, a high sensitivity alone does not make a test a perfect medical test. The test also needs to be negative for all cases without the disease. This ability is described by the specificity of the test. The specificity is the proportion of all patients without the disease and a negative test result (TN) of all those without the disease (TN + FP). The sensitivity and specificity can be formulated as follow:

$$Sensitivity = \frac{TP}{TP + FN} \tag{11}$$

$$Specifity = \frac{TN}{TN + FP} \tag{12}$$

The BWOA should find optimal values of ConvNet and SVM parameters with the aim of increasing the recognition accuracy. At the same time, the proposed method must have high sensitivity and specificity.

4 Results

In this section, the performance of the proposed method is evaluated. For this purpose, several experiments were performed and the obtained results are presented in the following subsections.

4.1 Dataset

In this study, the chest CT images dataset collected in the National Research Institute of Tuberculosis and Lung Diseases (NRITLD), Masih Daneshvari Hospital, Tehran, Iran is used for evaluation of the developed method [45]. The dataset is collected by three experienced radiologists with 15, 10, and 17 years of clinical experience between September 2019 and July 2020. This dataset includes 2688 CT slices from 336.

From 336 cases, 215 cases are patients confirmed with COVID-19 (1720 slices) and 121 cases are patients with other respiratory diseases such as Pneumonia, Emphysema, and Asthma that are confirmed by an experienced radiologist (968 slices). The 121 cases with other respiratory diseases were collected between September 2019 and January 2020 and COVID-19 cases are collected after the beginning of the outbreak. In COVID-19 cases, imaging studies were performed between 3-5 days from the onset of flu-like symptoms. All CT image slices of patients were converted to the gray-scale and resized to $256 \times 256 \times 1$ pixels. Table 1 lists the details of the dataset.

Table 1: Details of dataset [45]

Class	Gender	No. Cases	Age range	Age mean	Age SD
COVID-19	Male	96	[19 74]	46.3	15.8
	Female	119	[23 78]	51.2	12.4
Other respiratory diseases	Male	73	[19 77]	42.9	18.3
	Female	48	[18 75]	49.6	11.7

Figsures 8 and 9 show some CT images related to COVID-19 infected and COVID-19 not infected cases as an example. Figure 8 belongs to a 58-year-old woman who had a high fever for five days with a non-wet cough. In this case, the RT-PCR test was negative, but CT images indicated some areas of GGO and massive consolidation in the posterior parts of the lower lobes. The passage of time and further symptoms of the disease showed that this person was indeed suffering from the COVID-19. Moreover, Figure 9 shows CT images of a person with Pneumonia.

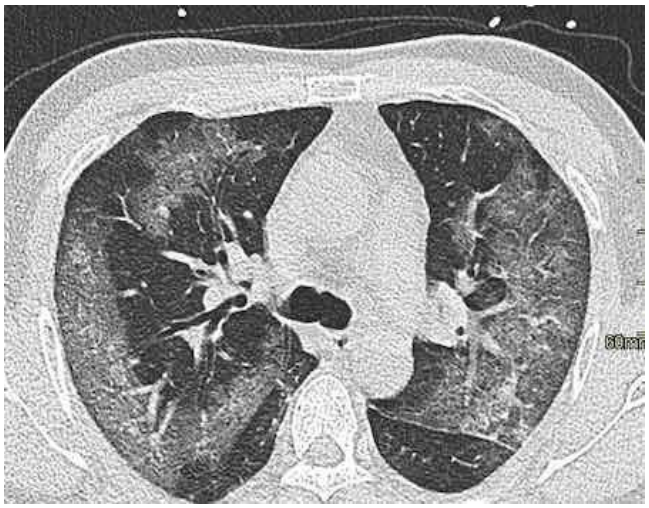

Figure 8. CT images of a person with COVID-19 in the dataset [45]

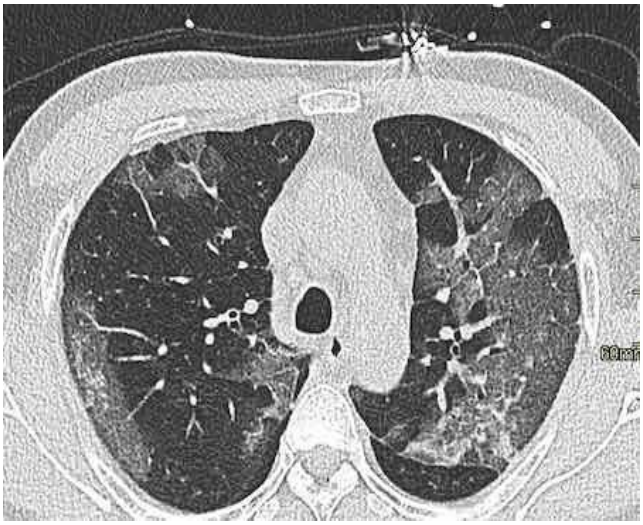

Figure 9. CT images of a person with Pneumonia [45]

All the obtained results are the average of 50 independent runs. The simulations are performed using a personal computer with five processing cores (core i7) and 16 GB RAM and Python programming language.

4.2 Performance of the proposed method

In this subsection, the performance of the proposed method is evaluated. For this purpose, hyper-parameters are selected using the optimization algorithm. In the BWOA, 20 spiders are generated randomly in the search space and the optimization process is iterated 100 times. The selected hyper-parameters using the BWOA are listed in Table 2. Based on the best obtained results, SVM with Gaussian radial basis function (GRBF) led to the highest recognition accuracy.

Therefore, we used this type of kernel function in the simulations. According to the BWOA, ConvNet with five layers (NL=5) and learning rate equal to 0.00164 ($\eta = 0.00164$) and SVM with $\gamma = 0.0539$ and C= 23.1 lead to the best performance.

Figure 10 shows the main structure of the developed COVID-19 diagnosis system. In the developed method, 1152 deep features are extracted using ConvNet. In the following module, feature selection module, the most efficient and informative features, 82 features, are selected out of 1152 features.

Table 2. Optimal configuration

Layer	Output shape	T_{Act}	NK_c	SK_c	S_c	Z	$T_{pooling}$	SK_p	S_p
Raw data	$256\times256\times1$	–	–	–	–	–	–	–	–
First	$123\times123\times3$	RReLU	32	6×6	2	1	L_p	3×3	1
Second	$118\times118\times64$	PReLU	64	5×5	1	1		2×2	1
Third	$56\times56\times128$	PReLU	128	4×4	2	2	Mixed	3×3	1
Fourth	$12\times12\times256$	PReLU	256	4×4	1	1	L_p	3×3	1
Fifth	$3\times3\times128$	RReLU	128	6×6	1	1	L_p	2×2	1
Flatten layer	1152×1	-	-	-	-	-	-	-	-
mRMR	82×1	-	-	-	-	-	-	-	-
SVM	$\gamma = 0.0539$	C=23.1	-	-	-	-	-	-	-

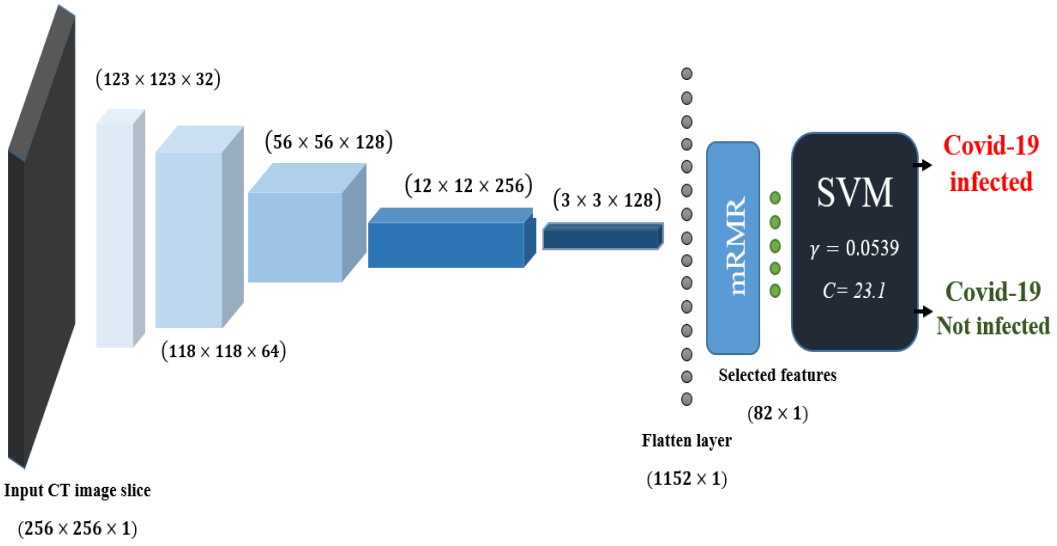

Figure 10. Main structure of developed COVID-19 diagnosis system

For examining the performance and generalization capability of our method, we have utilized different training/ validation/test ratios as listed by Table 3. For medical issues where data collection is difficult, the classifier should be able to train with a small amount of data and perform well on test data. In other words, it must have good generalization performance.

Table 3. Different Training/ Validation/Test sets (%)

Set	Training	Validation	Test
Set_1	30	10	60
Set_2	45	10	45
Set_3	60	10	30

Table 4 shows the performance of different optimized classifiers on test data. This table also shows the performance of conventional ConvNet, which combines convolutional layers with FLCs. In this case, all the hyper-parameters are optimized by BWOA. The obtained results demonstrate the superior performance of the developed method (BWOA – ConvNet – mRMR - SVM).

Table 4. Performance of the optimized classifiers on test data

Set	Classifier	Input	RA (%)	Sensitivity (%)	Specificity (%)	AUC
Set_1	FCL	1152×1	98.21	98.28	98.04	0.991
Set_1	FCL	82×1	98.47	98.56	98.22	0.991
Set_1	SVM	1152×1	99.04	99.14	98.75	0.992
Set_1	**SVM**	82×1	**99.37**	**99.42**	**99.29**	**0.996**
Set_2	FCL	1152×1	98.63	98.72	98.34	0.992
Set_2	FCL	82×1	99.17	99.23	99.05	0.993
Set_2	SVM	1152×1	99.25	99.36	99.05	0.994
Set_2	**SVM**	82×1	**99.66**	**99.74**	**99.54**	**0.997**
Set_3	FCL	1152×1	98.54	98.56	98.40	0.991
Set_3	FCL	82×1	99.07	99.14	98.93	0.992
Set_3	SVM	1152×1	99.18	99.28	98.93	0.993
Set_3	**SVM**	82×1	**99.53**	**99.57**	**99.46**	**0.996**

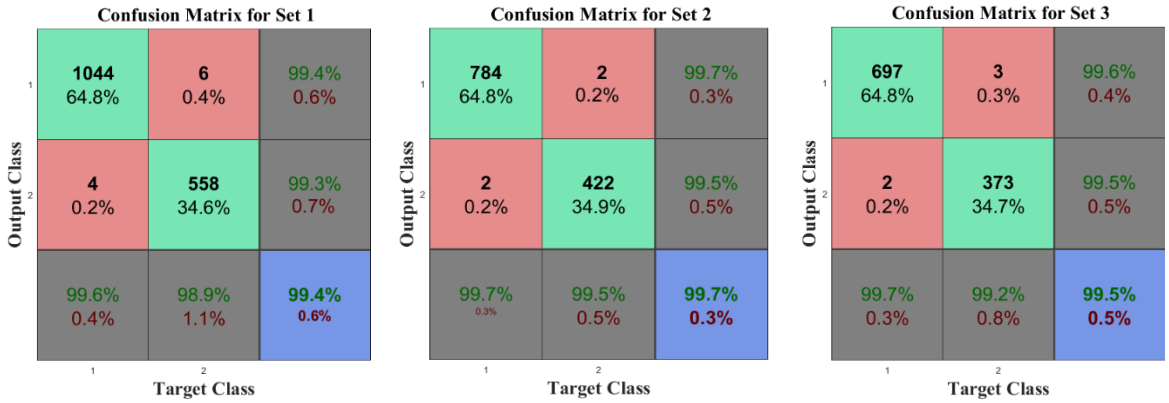

Figure 11. Confusion matrix of proposed method for different sets

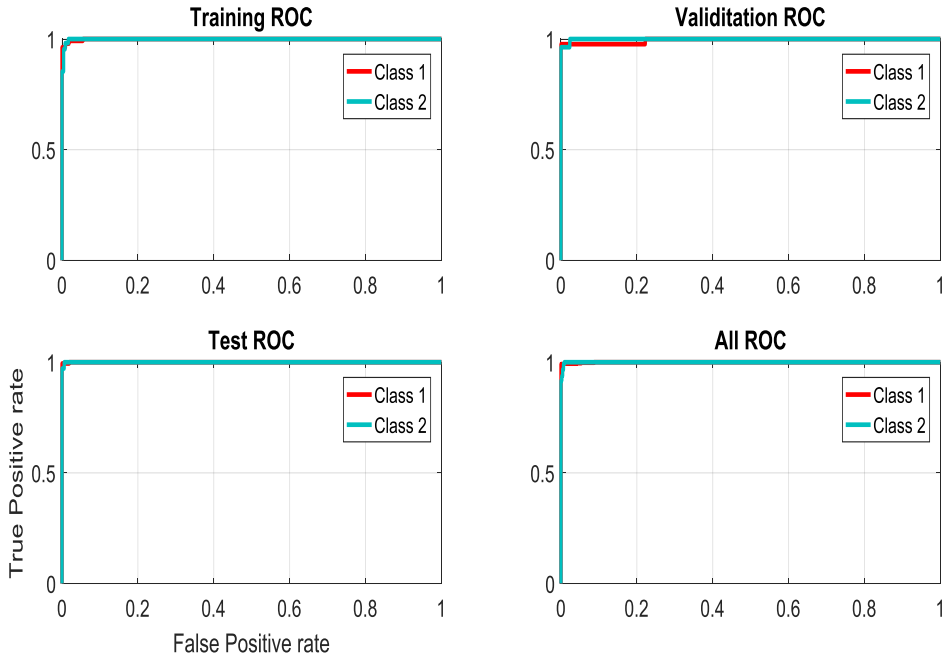

Figure 12. The ROC curves of the proposed method for Set 2

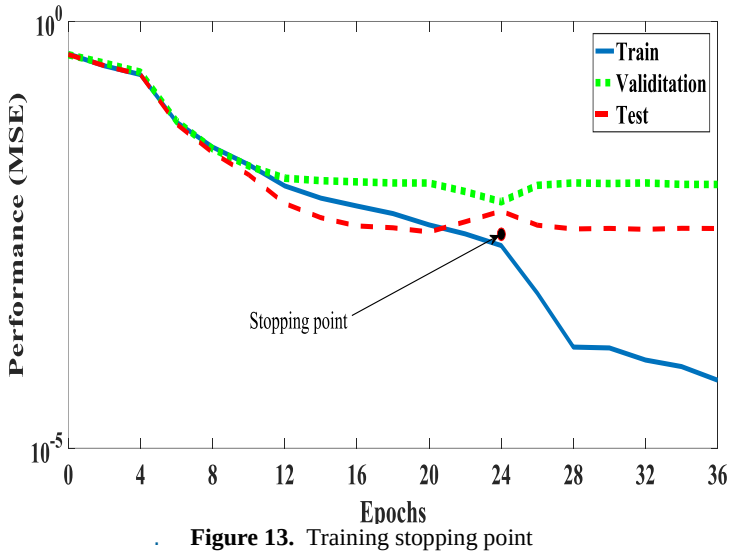

Figure 13. Training stopping point

For Set 1 that uses only 30% of data for training purpose, the developed method had 99.37% recognition accuracy. The results from these applications indicate that SVM classifiers exhibit enhanced generalization performance, which seems to be the power of support vector machines. Additionally, the AUC values are also calculated according to the area under the receiver operating characteristic (ROC) curves, if the AUC is close to one, it indicates an excellent classifier. For Set 2, the proposed classifier achieved AUC of 0.997, sensitivity, 99.74%; specificity, 99.54%; and accuracy, 99.66%. For Set 3 that uses large amount of data for training, the generalization capability is reduced a little.

Figure 11 shows confusion matrix of proposed method for different sets. Moreover, the obtained results show the high effect of feature selection algorithm performance of SVM. For example for Set 2, SVM using all extracted deep features (1152 features) and only selected features using mRMR (82 features) had 99.25% and 99.66% recognition accuracy, which prove the high impact of intelligent feature selection. Figure 12 the ROC curves for Set 2 and Figure 13 shows the training stopping point.

4.3 Discussion

For further investigations, the effect of hyper-parameters on ConvNet-SVM is investigated. In the first experiment, the effect of NL and ŋ is investigated on Set 2. For this purpose, several ConvNet-SVM with different NL and ŋ have been built and other hyper-parameters are optimized by BWOA. Figure14 shows the obtained results.

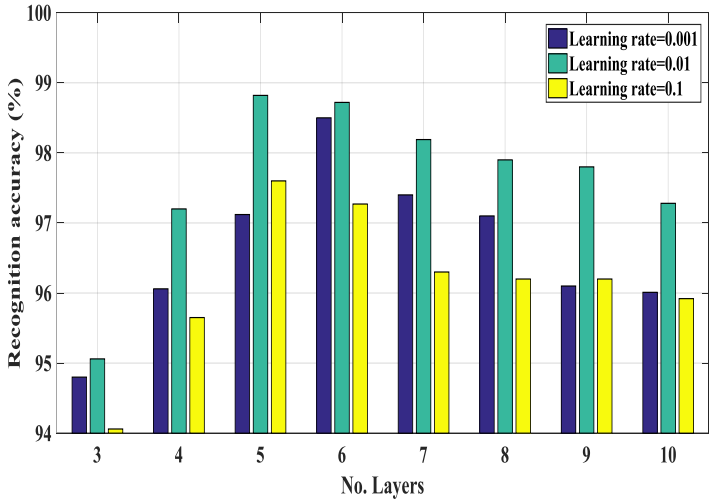

Figure 14. Effect of NL and ŋ on ConvNet-SVM performance

This figure shows that hyper-parameters such as NL and ŋ have a high impact on ConvNet-SVM accuracy. For instance, if the ŋ is very small, the algorithm may be get trapped in the local minimum. On the other hand, if the ŋ is very large, the algorithm cannot perform a good local search and derive the exact answer from the optimal point neighborhood. The NL has a high impact on the effectiveness of the extracted features. Using the low number of layers, hidden patterns in the input signal cannot be detected. On the other hand, if the number of layers is too high, it causes features to be extracted that have lost much useful information. This test shows that the depth of the network plays an important role. Of course, there is no direct and linear relationship between the number of layers and the degree of effectiveness of the features, and this hyper-parameter must be selected based on extensive simulations or optimization algorithms. Similar conditions exist for other hyper-parameters such as the number of filter in ConvNet, and their value must be carefully selected to ensure the network performs best.

In the next experiment, the effect of γ and C on SVM performance are investigated using Set 2. In this experiment, the hyper-parameters of ConvNet are optimized by BWOA. The obtained results are listed in Table V. It can be seen that there are no straight relationship between the value of γ and C, and SVM performance. For example, we cannot say that increasing the value of γ increase the recognition accuracy. Therefore, the value of these parameters should be determined carefully.

Table 5. Effect of SVM hyper-parameters using Set 2

γ	C	RA (%)
0.01	0.1	98.35
0.1	10	98.60
1	100	97.69
10	1000	97.11
0.01	1000	98.35
0.1	100	98.31
1	10	97.38
10	1	97.02

One of the important characteristics that each classifier must have is the same performance in different implementations. In other words, the classifier must have robust performance. To investigate the robustness of the proposed method in different implementations, the proposed method was run 50 times and simulation results showed that the standard deviation (SD) of the algorithm was zero. This value indicates that the proposed method can be reliably applied to different data and yields excellent results. In Figure 15, the convergence of the BWOA is shown in three different independent implementations. It can be seen that in all three implementations, the algorithm converges to the same accuracy and has a robust performance. In addition, this figure shows the changes in the learning rate parameter during the optimization process as an example of BWOA performance.

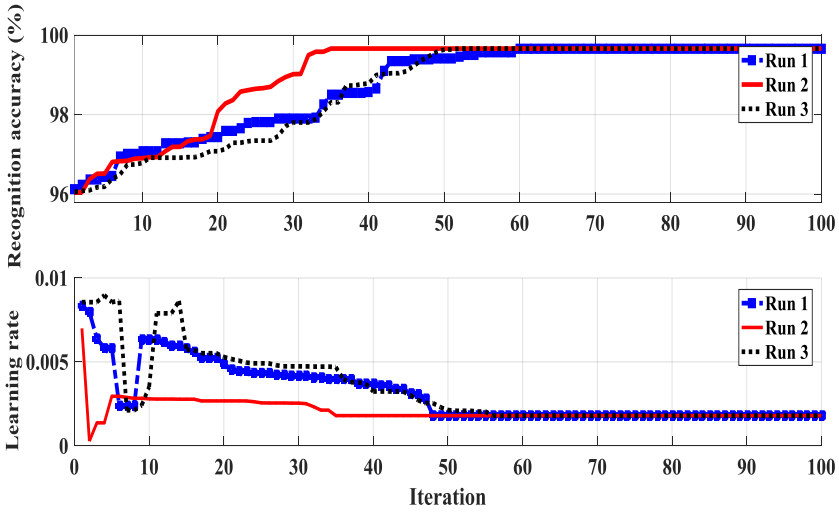

Figure 15. BWOA convergence

Recently, early detection of COVID-19 has been attracted lots of attentions among the researchers and scientists so that various studies have been done in this case due to the importance of COVID-19 accurate diagnosis. Since there is no single dataset available, then comparing with other methods directly is kind of a difficult task for COVID-19 detection problem. Setting the patterns differently (for example, the number of training and testing samples and the number of patterns) provides us with various performance. Due to some facts such as different CT scan devices which may give different CT images with different qualities, and also the relationship among race and COVID-19 mortality and infection which may give various trends, then the direct numerical comparison will become very difficult. In the comparison stage, two newly emerged approaches available in the literature have been employed on our dataset. The obtained results are listed in Table 6. All the listed results are the average of 50 independent runs.

This experiment proves the high generalization performance of the proposed method. For Set 1, the highest accuracy, 99.37% is achieved by proposed method. The other classifiers much lower accuracy than our method. Moreover, this experiment proves the superiority of SVM over other classifiers like LSTM and FCL.

Table 6. Performance analysis of various methods

Ref	Method	Structure	Set	RA (%)
[18]	ConvNet	ResNet-101	1	99.01
[18]	ConvNet	Xception	1	98.82
[19]	ConvNet	Pre-trained ResNet18	1	98.47
[19]	ConvNet	Pre-trained ResNet50	1	98.62
[19]	ConvNet	Pre-trained SqueezeNet	1	98.49
[21]	ConvNet + LSTM	Trial and error	1	98.93
This study	ConvNet + SVM	Optimized by BWOA	1	99.37
[18]	ConvNet	ResNet-101	2	99.36
[18]	ConvNet	Xception	2	99.21
[19]	ConvNet	Pre-trained ResNet18	2	99.09
[19]	ConvNet	Pre-trained ResNet50	2	99.13
[19]	ConvNet	Pre-trained SqueezeNet	2	99.05
[21]	ConvNet + LSTM	Trial and error	2	99.27
This study	ConvNet + SVM	Optimized by BWOA	2	99.66
[18]	ConvNet	ResNet-101	3	99.32
[18]	ConvNet	Xception	3	99.24
[19]	ConvNet	Pre-trained ResNet18	3	98.78
[19]	ConvNet	Pre-trained ResNet50	3	98.94
[19]	ConvNet	Pre-trained SqueezeNet	3	99.02
[21]	ConvNet + LSTM	Trial and error	3	99.18
This study	ConvNet + SVM	Optimized by BWOA	3	99.53

5 Conclusion

The number of cases of COVID-19 continues to rise in Iran and around the world. In this condition, timely diagnosis of the disease in early stages can help physicians to adopt the right decisions and choose appropriate remedies methods, and ultimately increase the chances of survival of the patient to a very high level. According to the importance of the issue, in this study, a new hybrid method was presented to process a CT scan of chest images and diagnosis of COVID-19 disease. In this method, the ConvNet was used for the automatic extraction of characteristics and the SVM for the final classification of images. In addition, mRMR was used for feature selection and BWOA was used to select the optimal parameters of ConvNet and the SVM. The proposed method can diagnose the disease with high accuracy.

Besides the high recognition accuracy, the proposed method has high sensitivity and specificity and is recommended for patients with early COVID-19 stage. The developed method can be useful in eliminating disadvantages such as an insufficient number of available RT-PCR test kits, test costs, and waiting time of test results. Application of the proposed COVID-19 diagnosis system can be helpful for the accurate and early detection of this disease, and can also be assistive to overcome the

challenge of a lack of specialized physicians in remote villages. According to simulation results, the developed method can be trained properly without needing for large amount of database.

Acknowledgment: The authors would like to thank Dr. Ali Vahedi for providing the data.

Conflicts of Interest: The authors declare that they have no conflicts of interest to report regarding the present study.

References

[1] Coronavirus disease (COVID-2019) situation reports, World Health Organization. https://www.who.int. [Accessed June 2020]

[2] A. Xiao, Y. Tonga, C. Gao, L. Zhu, Y. Jie, and Z. Zhang, "Dynamic profile of RT-PCR findings from 301 COVID-19 patients in Wuhan, China: A descriptive study," *Journal of Clinical Virology*, vol. 127, Article 104346, 2020.

[3] G. Singer, and M. Marudi, "Ordinal Decision-Tree-Based Ensemble Approaches: The Case of Controlling the Daily Local Growth Rate of the COVID-19 Epidemic," *Entropy*, vol. 22, no. 8, pp. 871, 2020.

[4] C. Long, H. Xu, Q. Shen, X. Zhang, B. Fan, C. Wang, B. Zeng, Z. Li, X. Li, and H. Li, "Diagnosis of the Coronavirus disease (COVID-19): rRT-PCR or CT?," *European Journal of Radiology*, vol. 126, Article. 108961, 2020.

[5] S. Liu, Y. Liu, and Y. Liu, "Somatic symptoms and concern regarding COVID-19 among Chinese college and primary school students: A cross-sectional survey," *Psychiatry Research*, vol. 289, Article. 113070, 2020.

[6] M. El Homsi, M. Chung, A. Bernheim, A. Jacobi, M. King, S. Lewis, and B. Taouli, "Review of chest CT manifestations of COVID-19 infection," *European Journal of Radiology Open*, vol. 7, Article. 100239, 2020.

[7] T. Ozturk, M. Talo, E. Azra Yildirim, U. Baran Baloglu, O. Yildirim, U.R. Acharya, "Automated detection of COVID-19 cases using deep neural networks with X-ray images," *Computers in Biology and Medicine*, vol. 121, Article. 103792, 2020.

[8] J.F.W. Chan, S. Yuan, K.H. Kok, K.K.W. To, H. Chu, G. Yang, and et al, "A familial cluster of pneumonia associated with the 2019 novel coronavirus indicating person-to-person transmission: a study of a family cluster," *Lancet*, vol. 395, no. 10223, pp. 514-523, 2020.

[9] A. Hamimi, "MERS- CoV: Middle East respiratory syndrome corona virus: Can radiology be of help? Initial single center experience," *The Egyptian Journal of Radiology and Nuclear Medicine*, vol. 47, no. 1, pp. 95-106, 2016.

[10] H. Chen, Q. Zhang, J. Luo, Y. Xu, and X Zhang, "An enhanced Bacterial Foraging Optimization and its application for training kernel extreme learning machine," *Applied Soft Computing*, vol. 86, Article. 105884, 2020.

[11] L. Shen, H. Chen, Z. Yu, W. Kang, B. Zhang, H. Li, B. Yang, and D. Liu, "Evolving support vector machines using fruit fly optimization for medical data classification," *Knowledge-Based Systems*, vol. 96, pp. 61-75, 2016.

[12] M. Wang, and H. Chen, "Chaotic multi-swarm whale optimizer boosted support vector machine for medical diagnosis," *Applied Soft Computing*, vol. 88, 105946, 2020.

[13] P. Zarbakhsh, and A. Addeh, "Breast cancer tumor type recognition using graph feature selection technique and radial basis function neural network with optimal structure," *Journal of Cancer Research and Therapeutics*, vol. 14, pp. 625-633, 2020.

[14] X. Xu, and H.L. Chen, "Adaptive computational chemotaxis based on field in bacterial foraging optimization," *Soft Computing*, vol. 18, no. 4, pp. 797-807, 2014.

[15] Y. Xu, H. Chen, J. Luo, Q. Zhang, S. Jiao, and X. Zhang, "Enhanced Moth-flame optimizer with mutation strategy for global optimization," *Information Sciences*, vol. 492, pp. 181-203, 2019.

[16] X. Zhao, D. Li, B. Yang, C. Ma, Y. Zhu, and H. Chen, "Feature selection based on improved ant colony optimization for online detection of foreign fiber in cotton," *Applied Soft Computing*, vol. 24, pp. 585-596, 2014.

[17] X. Zhao, X. Zhang, Z. Cai, X. Tian, X. Wang, Y. Huang, H. Chen, and L. Hu, "Chaos enhanced grey wolf optimization wrapped ELM for diagnosis of paraquat-poisoned patients," *Computational Biology and Chemistry*, vol. 78, pp. 481-490, 2019.

[18] A. Abbasian Ardakani, A. Rajabzadeh Kanafi, U.R. Acharya, N. Khadem, and A. Mohammadi "Application of deep learning technique to manage COVID-19 in routine clinical practice using CT images: Results of 10 convolutional neural networks," *Computers in Biology and Medicine*, vol. 121, Article 103795, 2020.

[19] S. Ahuja, B. Ketan Panigrahi, N. Dey, V. Rajinikanth, and T. Kumar Gandhi1, "Deep transfer learning-based automated detection of COVID-19 from lung CT scan slices," *Applied Intelligence*, pp. 1-15, 2020.

[20] K. Zhang, X. Liu, J. Shen, and et al, "Clinically applicable AI system for accurate diag- nosis, quantitative measurements, and prognosis of COVID-19 Pneumonia using computed tomography," *Cell*, vol. 181, no. 6, pp. 1423-1433, 2020.

[21] A. Hasan, M. AL-Jawad, H. Jalab, H. Shaiba, R. Ibrahim, and A. AL-Shamasneh, "Classification of Covid-19 Coronavirus, Pneumonia and Healthy Lungs in CT Scans Using Q-Deformed Entropy and Deep Learning Features," *Entropy*, vol. 22, pp. 517, 2020.

[22] L. Li, L. Qin, Z. Xu, and et al, "Artificial intelligence distinguishes COVID-19 from community acquired pneumonia on chest CT," *Radiology*, vol. 296, no. 2, Article. 200905, 2020.

[23] X. Ouyang, J. Huo, L. Xia, and et al, "Dual-sampling attention network for diagnosis of COVID-19 from community acquired Pneumonia," *IEEE Trans Med Imaging*, vol. 39, no. 8, 39 (8), Article .2995508, 2020.

[24] S. Christodoulidis, M. Anthimopoulos, L. Ebner, A. Christe, and S. Mougiakakou, "Mul- tisource transfer learning with convolutional neural networks for lung pattern analysis," *IEEE J Biomed Health Inform*, vo. 21, pp. 76–84, 2017.

[25] S. Ahmad Qureshi, and A. ul Rehman, "Computed Tomography, Deep Learning and Ultrasonography Role in the Diagnosis of COVID-19 Pendemic Lung Infection," *Photodiagnosis and Photodynamic Therapy*, vol. 31, Article 101880, 2020.

[26] L. Brunese, F. Mercaldo, A. Reginelli, and A. Santone, "Explainable Deep Learning for Pulmonary Disease and Coronavirus COVID-19 Detection from X-rays," *Computer Methods and Programs in Biomedicine*, vol. 196, Article. 105608, 2020.

[27] M. Toğaçar, B. Ergen, and Z. Cömert, "COVID-19 detection using deep learning models to exploit Social Mimic Optimization and structured chest X-ray images using fuzzy color and stacking approaches," *Computers in Biology and Medicine*, vol. 121, Article. 103805, 2020.

[28] H. Panwar, P.K. Gupta, M. Khubeb Siddiqui, R. Morales-Menendez, and V. Singh, "Application of deep learning for fast detection of COVID-19 in X-Rays using nCOVnet," *Chaos, Solitons & Fractals*, vol. 138, Article. 109944, 2020.

[29] D. Singh, V. Kumar, V. Kaur, and M. Kaur, "Classification of COVID-19 patients from chest CT images using multi-objective differential evolution–based convolutional neural networks," *European Journal of Clinical Microbiology & Infectious Diseases*, vol. 39, p.p. 1379–1389, 2020.

[30] T. BurakAlakus, and I. Turkoglu, "Comparison of deep learning approaches to predict COVID-19 infection," *Chaos, Solitons & Fractals*, vol. 140, Article. 110120, 2020.

[31] X. Wu, H. Hui, M. Niu, L. Li, L. Wang, B. He, X. Yang, L. Li, H. Li, J. Tian, and Y. Zha, "Deep learning-based multi-view fusion model for screening 2019 novel coronavirus pneumonia: A multicentre study," *European Journal of Radiology*, vol. 128, Artivle. 109041, 2020.

[32] C. Jalaber, T. Lapotre, T. Morcet-Delattre, F. Ribet, S. Jouneau, and M. Lederlin, "Chest CT in COVID-19 pneumonia: A review of current knowledge," *Diagnostic and Interventional Imaging*, vol. 101, p.p. 431-437, 2020.

[33] N. A. Golilarz, A. Addeh, H. Gao, L. Ali, A. Moradkhani Roshandeh, H. Mudassir Munir, and R. U. Khan, "A New Automatic Method for Control Chart Patterns Recognition Based on ConvNet and Harris Hawks Meta Heuristic Optimization Algorithm," *IEEE Access*, vol. 7, pp. 149398-149405, 2019.

[34] N. Amiri Golilarz, H. Gao, R. Kumar, L. Ali, Y. Fu, C. Li, "Adaptive Wavelet Based MRI Brain Image De-noising," *Frontiers in Neuroscience*, vol. 14:728, 2020.

[35] M. Véstias, "A Survey of Convolutional Neural Networks on Edge with Reconfigurable Computing," *Algorithms*, vol. 12, p.p. 154, 2019.

[36] M. Izadpanahkakhk, S.M. Razavi, M. Taghipour-Gorjikolaie, S.H. Zahiri, and A. Uncini, "Deep Region of Interest and Feature Extraction Models for Palmprint Verification Using Convolutional Neural Networks Transfer Learning," *Appl. Sci*, vol. 8, p.p. 1210, 2018.

[37] Z. Tan, P. Yue, L. Di, and J. Tang, "Deriving High Spatiotemporal Remote Sensing Images Using Deep Convolutional Network," *Remote Sens*, vol. 10, p.p. 1066, 2018.

[38] F. Zhou, P. Hu, S. Yang, and C. Wen, "A Multimodal Feature Fusion-Based Deep Learning Method for Online Fault Diagnosis of Rotating Machinery," *Sensors*, vol. 18, p.p. 3521, 2018.

[39] N. Yuan, W. Yang, B. Kang, S. Xu, and X. Wang, "Laplacian Eigenmaps Feature Conversion and Particle Swarm Optimization-Based Deep Neural Network for Machine Condition Monitoring," *Appl. Sci*, vol. 8, p.p. 2611, 2018.

[40] M. Behzad, K. Asghari, M. Eazi, and M. Palhang, "Generalization performance of support vector machines and neural networks in runoff modeling," *Expert Systems with Applications*, vol. 36, p.p. 7624- 7629, 2009.

[41] V. Hayyolalam, and A. Pourhaji Kazem, "Black Widow Optimization Algorithm: A novel meta-heuristic approach for solving engineering optimization problems," *Engineering Applications of Artificial Intelligence*, vol. 87, Article. 103249, 2020.

[42] Q. Yang, Q. Liu, H. Xu, H. Lu, S. Liu, and H. Li, "Imaging of coronavirus disease 2019: A Chinese expert consensus statement," *European Journal of Radiology*, vol. 127, Article 109008, 2020.

[43] X. Zhao, B. Liu, Y. Yu, X. Wang, Y. Du, J. Gu, and X. Wu, "The characteristics and clinical value of chest CT images of novel coronavirus pneumonia," *Clinical Radiology*, vol. 75, p.p. 335-340, 2020.

[44] J. Gu, Z. Wang, J. Kuen, L. Ma, A. Shahroudy, B. Shuai, T. Liu, X. Wang, G. Wang, J. Cai, and T. Chen, "Recent advances in convolutional neural networks," *Pattern Recognition*, vol. 77, p.p. 354-377, 2018.

[45] National Research Institute of Tuberculosis and Lung Diseases (NRITLD), Masih Daneshvari Hospital. http://en.nritld.sbmu.ac.ir/index.jsp?fkeyid=&siteid=201&pageid=39854

[46] M. Shahid et al., "Wavelet Based Image DE-Noising with Optimized Thresholding Using HHO Algorithm," 16th International Computer Conference on Wavelet Active Media Technology and Information Processing, Chengdu, China, 2019.

[47] A. Addeh et al., "Control chart pattern recognition using RBF neural network with new training algorithm and practical features," *ISA Transactions*, vol. 79, pp. 202-216, 2018.

[48] A. A. Heidari, S. Mirjalili, H. Faris, I. Aljarah, M. Mafarja, and H. Chen, "Harris hawks optimization: Algorithm and applications,"' *Future Generation Computer Systems*, vol. 97, no. 3, pp. 849-872, 2019.